

Measurement of charm production cross
sections in e^+e^- annihilation
at energies between 3.97 and 4.26 GeV

Gu Shan

2018.1.8

JC 48 report

Introduction

- Little intensive study about hadron production in electron-positron annihilations just above $c\bar{c}$ threshold.
- Any comprehensive program of precise charm-decay measurements demands a detailed understanding of charm production.
- There is a rich structure in this energy region, reflecting the production of $c\bar{c}$ resonances and the crossing of thresholds for specific charm-meson final states.
- Considerable theoretical interest and little experimental information .

Data sets and decay modes

TABLE I. Center-of-mass energies and integrated luminosity totals for all data samples used in this paper.

$E_{\text{c.m.}}$ (MeV)	$\int \mathcal{L} dt$ (pb $^{-1}$)
3970	3.85
3990	3.36
4010	5.63
4015	1.47
4030	3.01
4060	3.29
4120	2.76
4140	4.87
4160	10.16
4170	178.89
4180	5.67
4200	2.81
4260	13.11

$$D^0 \rightarrow K^- \pi^+$$

$$D^+ \rightarrow K^- \pi^+ \pi^+$$

$$D_S:$$

Modes	Reference	\mathcal{B} (%)
$K^+ K^- \pi^+, M_{KK} - M_\phi < (10 \text{ MeV}/c^2)$	[15]	1.99 ± 0.11
$\bar{K}^{*0} K^+, \bar{K}^{*0} \rightarrow K^- \pi^+$	[5]	2.2 ± 0.6
$\eta \pi^+, \eta \rightarrow \gamma\gamma$	[5,15]	0.62 ± 0.08
$\eta \rho^+, \eta \rightarrow \gamma\gamma, \rho^+ \rightarrow \pi^+ \pi^0$	[5]	4.3 ± 1.2
$\eta' \pi^+, \eta' \rightarrow \pi^+ \pi^- \eta, \eta \rightarrow \gamma\gamma$	[5,15]	0.66 ± 0.07
$\eta' \rho^+, \eta' \rightarrow \pi^+ \pi^- \eta, \eta \rightarrow \gamma\gamma, \rho^+ \rightarrow \pi^+ \pi^0$	[5]	1.8 ± 0.5
$\phi \rho^+, \phi \rightarrow K^+ K^-, \rho^+ \rightarrow \pi^+ \pi^0$	[5]	3.4 ± 1.2
$K_S K^+, K_S \rightarrow \pi^+ \pi^-$	[5,15]	1.03 ± 0.06

MC simulation

$$\Delta E \equiv E_{D(s)} - E_{\text{beam}}$$

$$M_{\text{bc}} \equiv \sqrt{E_{\text{beam}}^2 - |\mathbf{P}_{D(s)}|^2}$$

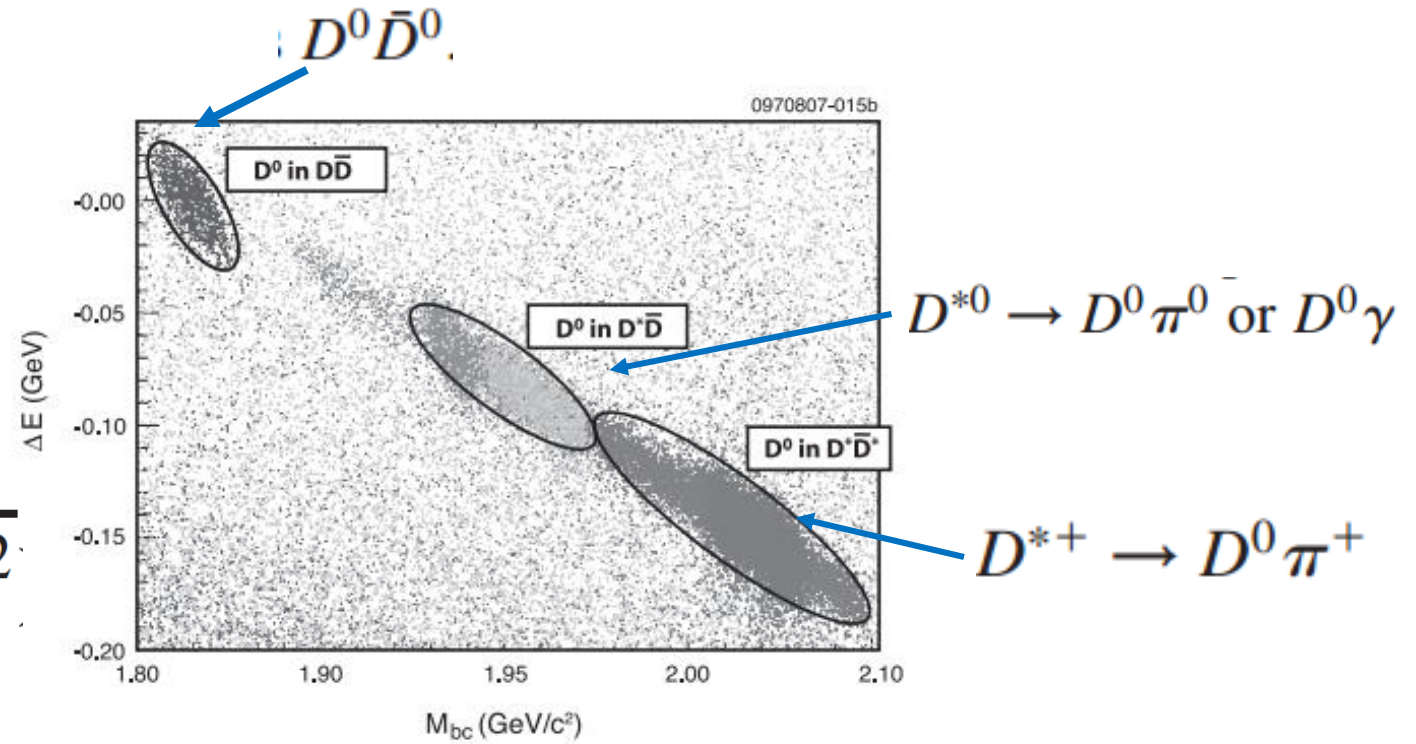


FIG. 1. ΔE vs M_{bc} for $D^0 \rightarrow K^- \pi^+$ candidates in a Monte Carlo simulation of CLEO-c data at a center-of-mass energy of 4160 MeV. Separation among the expected two-charm-meson final states is evident, as described in the text.

Momentum spectra

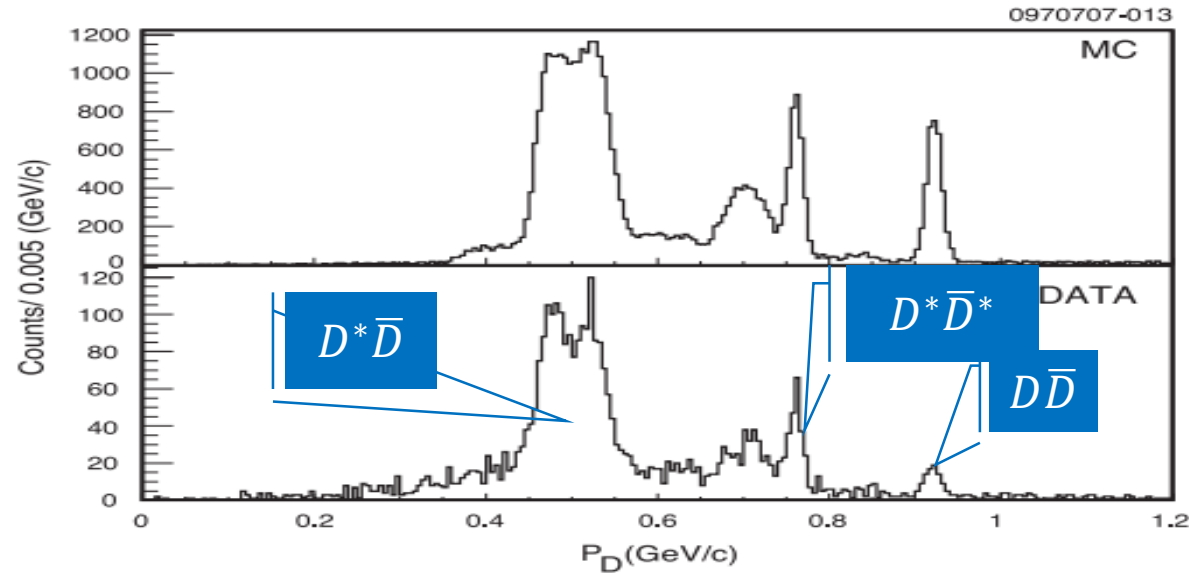


FIG. 2. Momentum spectra in Monte Carlo simulation (top) and data (bottom) at 4160 MeV for $D^0 \rightarrow K^- \pi^+$ candidates with invariant masses within 15 MeV of the nominal value. There is reasonable agreement between the Monte Carlo simulation and data, with clear peaks corresponding to the expected final states with two charm mesons at this energy ($D\bar{D}$, $D^*\bar{D}$ and $D^*\bar{D}^*$). Quantitative interpretation of the momentum spectrum requires correction for non-charm-meson backgrounds, consideration of additional channels for charm-meson production, radiative effects, and other phenomena, as described in the text.

Fit

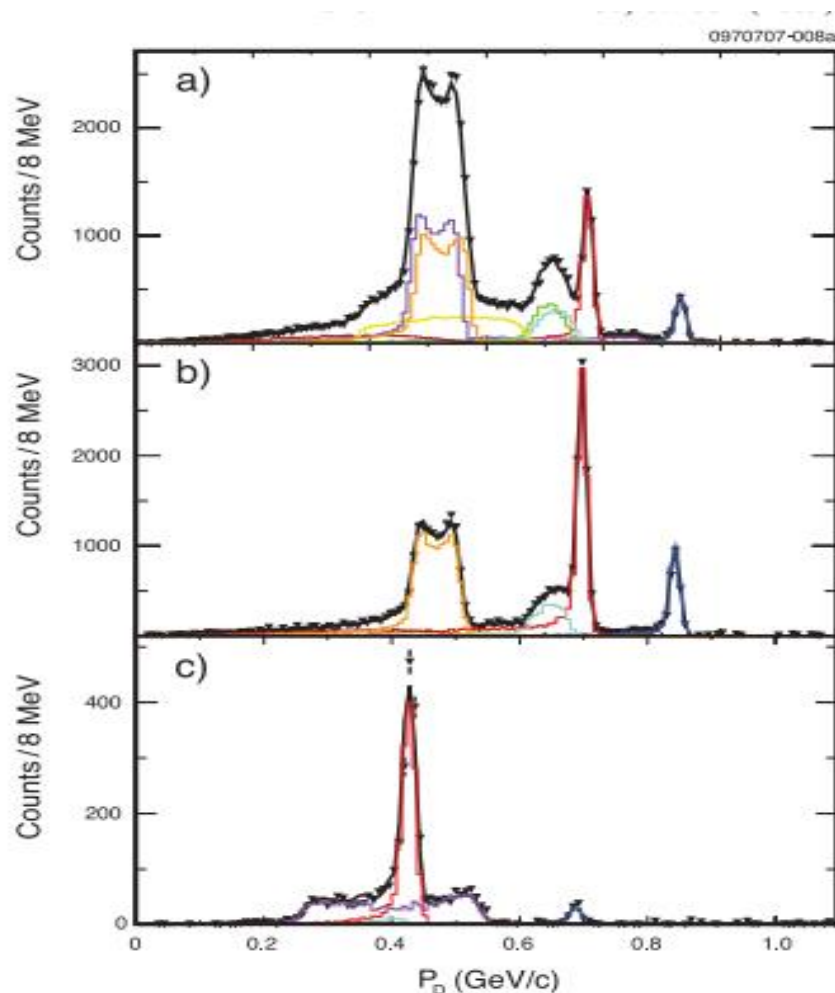
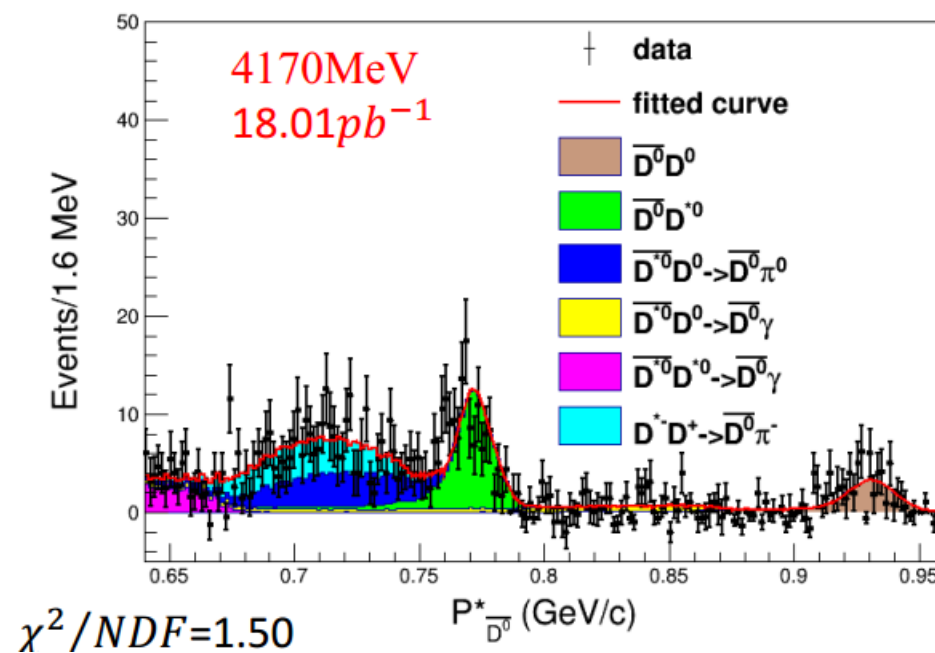


FIG. 4 (color). Sideband-subtracted momentum spectra for (a) $D^0 \rightarrow K^- \pi^+$, (b) $D^+ \rightarrow K^- \pi^+ \pi^+$, and (c) $D_s^+ \rightarrow \phi \pi^+$ at 4170 MeV. Data are shown as points with errors and the total fit result is shown as the solid black line. The colored histograms represent specific $D_{(s)}$ -production mechanisms, with shapes obtained from Monte Carlo simulations and normalizations determined by the fits. The color code for the components of the fits and the χ^2 values is given in the text.

4170 MeV

BES III



Fit

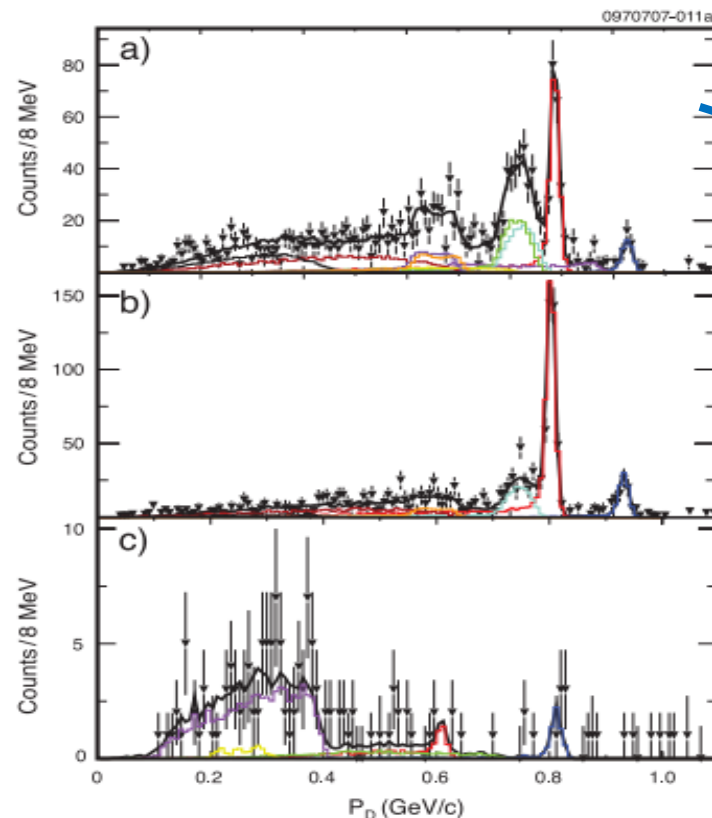
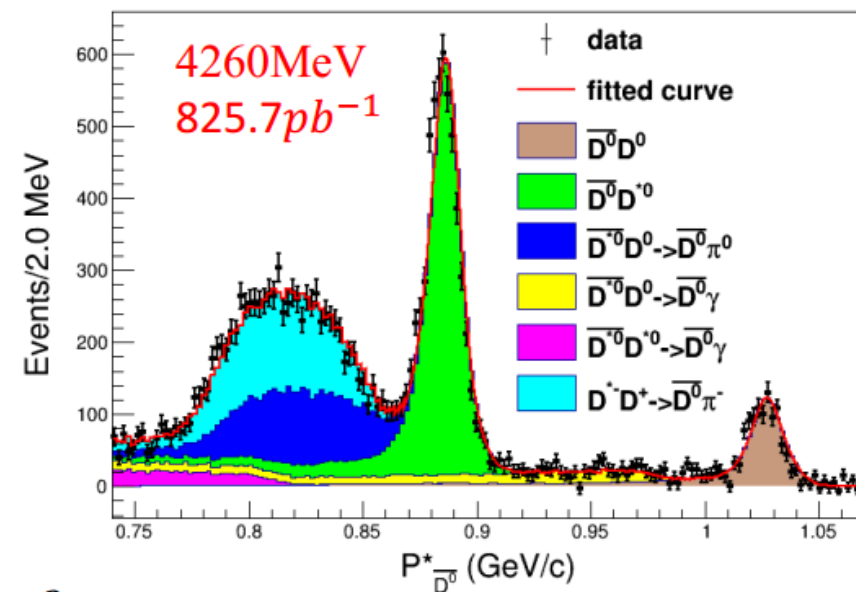


FIG. 5 (color). Sideband-subtracted momentum spectra for (a) $D^0 \rightarrow K^- \pi^+$, (b) $D^+ \rightarrow K^- \pi^+ \pi^+$, and (c) $D_s^+ \rightarrow \phi \pi^+$ at 4260 MeV. Data are shown as points with errors and the total fit result is shown as the solid black line. The colored histograms represent specific $D_{(s)}$ -production mechanisms, with shapes obtained from Monte Carlo simulations and normalizations determined by the fits. The color coding for the components matches that of Fig. 4, as described in the text. All peaks are shifted slightly higher in momentum, and the low-momentum region is populated by two multibody components: the $D^* \bar{D} \pi$ (dark red line) between 0 and 0.6 GeV/c, observed at 4170 MeV, and $D^* \bar{D}^* \pi$ (black line) between 0 and 0.4 GeV/c, which is not present at lower energy.

BES III



$$\chi^2/NDF=1.51$$

Cross section

None-ISR

TABLE IV. Measured cross sections for final states consisting of two neutral nonstrange charm mesons. The first error on each cross section is statistical and the second is systematic.

$E_{\text{c.m.}}$ (MeV)	$\sigma(D^0\bar{D}^0)$ (pb)	$\sigma(D^{*0}\bar{D}^0)$ (pb)	$\sigma(D^{*0}\bar{D}^{*0})$ (pb)
3970	$86 \pm 29 \pm 4$	$2280 \pm 134 \pm 78$...
3990	$133 \pm 41 \pm 6$	$2740 \pm 157 \pm 93$...
4010	$76 \pm 25 \pm 3$	$3320 \pm 13 \pm 113$...
4015	<10 (90% C.L.)	$3840 \pm 283 \pm 131$	$213 \pm 76 \pm 9$
4030	$334 \pm 70 \pm 15$	$3200 \pm 183 \pm 109$	$2000 \pm 125 \pm 94$
4060	$410 \pm 72 \pm 18$	$2230 \pm 147 \pm 76$	$2290 \pm 132 \pm 108$
4120	$303 \pm 70 \pm 14$	$1400 \pm 135 \pm 48$	$2550 \pm 154 \pm 120$
4140	$177 \pm 40 \pm 8$	$1350 \pm 100 \pm 46$	$2443 \pm 116 \pm 115$
4160	$167 \pm 28 \pm 8$	$1252 \pm 69 \pm 43$	$2566 \pm 84 \pm 121$
4170	$177 \pm 7 \pm 8$	$1272 \pm 19 \pm 43$	$2363 \pm 19 \pm 111$
4180	$179 \pm 39 \pm 8$	$1211 \pm 92 \pm 41$	$2173 \pm 104 \pm 102$
4200	$180 \pm 55 \pm 8$	$1030 \pm 123 \pm 35$	$1830 \pm 139 \pm 86$
4260	$86 \pm 18 \pm 4$	$1080 \pm 59 \pm 37$	$269 \pm 42 \pm 13$

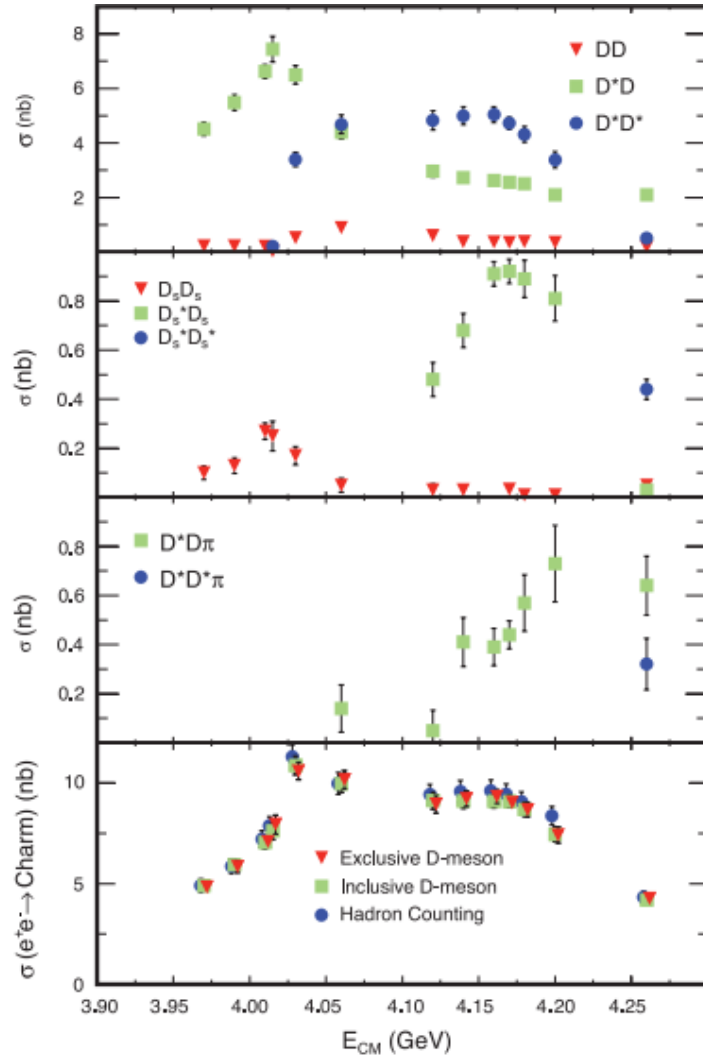


FIG. 6 (color). Exclusive cross sections for two-body and multibody charm-meson final states, and total observed charm cross section with combined statistical and systematic uncertainties.

BES III will give the result of cross sections with the ISR at energies between 3.89 and 4.6 GeV .

Some problems at BES III

- 664P01:KKMC-00-00-44/src/bornv/RRes.F
- :703: KKMC/KKMC-00-00-57/src/bornv/RRes.F
- By Like:
- <http://indico.ihep.ac.cn/event/4781/contribution/8/material/slides/0.pdf>

ConExc

xs_user.txt

3.8900	293.004	0
3.8909	295.978	0
3.8918	299.475	0
3.8927	303.487	0
3.8936	308.004	0
3.8944	313.019	0
3.8953	318.522	0
3.8962	324.504	0
3.8971	330.958	0
3.8980	337.872	0
3.8989	345.235	0
3.8998	353.039	0
3.9007	361.271	0
3.9016	369.922	0
3.9024	378.981	0
3.9033	388.437	0
3.9042	398.281	0
3.9051	408.502	0
3.9060	419.089	0
3.9069	430.033	0
3.9078	441.321	0

```
void EvtXsection::ini_data_diy(){//user provide xs list
xx.clear();yy.clear();er.clear();
ifstream file("xs_user.txt");
double xm,xs,xs_er;
while(!file.eof()){
file>>xm>>xs>>xs_er;
// std::cout<<"read XS: "<<xm<<" "<<xs<<" "<<xs_er<<std::endl;
xx.push_back(xm);
yy.push_back(xs);
er.push_back(xs_er);
}
xx.pop_back();
yy.pop_back();
er.pop_back();
nbins=yy.size();
file.close();
_unit="";
_msg="";
}
```

Here "vhdr" is the mandatory part of the ISR photon emission) decays to the

KMC

xs_user.dat

```
IF(ICH.EQ.-2) THEN
DO IJ=1,1000 !INITIALIZE ARRAY
USER_XX(IJ)=0
USER_YY(IJ)=0
ENDDO
NDIM = 0
OPEN(unit=91, FILE='./xs_user.dat', STATUS='old')
rewind 91
DO IJ=1,1000
NDIM = IJ
READ(91,*,end=100) USER_XX(NDIM),USER_YY(NDIM)
print*, USER_XX(NDIM)-C50_XX(NDIM),USER_YY(NDIM)-C50_YY(IJ)
ENDDO
NDIM = NDIM-1
IF(NDIM .EQ.1) THEN
PRINT*, 'NO DATA ACESIBLE IN THE FILE xs_user.dat'
STOP
ENDIF
youxs= XLININT(USER_YY,USER_XX,SQRS,NDIM)
XBORN= XLININT(USER_YY,USER_XX,CMS, NDIM)
ELSEIF(ICH .GE.0) THEN
youxs= XLININT(YY,XX,SQRS,N1)
XBORN= XLININT(YY,XX,CMS, N1)
ELSE
PRINT*, 'BAD MODE INDEX, I STOP'
STOP
ENDIF
```

82	$\pi^0\pi^0h_c$	4.009 ~4.42 GeV
90	$J/\psi\pi^+\pi^-$	3.82917 ~5.47083
91	$\psi(2S)\pi^+\pi^-$	4.12745 ~5.48039
92	$J/\psi K^+K^-$	4.17209 ~5.97674
93	$D^+D_s^-$	3.97 ~4.26 GeV
94	$D_s^+D_s^-$	4.12 ~4.26 GeV
95	$D_s^{*-}D_s^+$	4.12 ~4.26 GeV

\sqrt{s} GeV	4.19	4.21	4.22
KKMC	0.830	0.815	0.810
ConExc	0.826	0.813	0.808

THE ISR CORRECTION FACTOR COMPARISON

The ISR correction factors calculated in the generator model "ConExc" within the ISR correction factor calculated with the model "KKMC" for the process $e^+e^- \rightarrow \pi^+\pi^- J/\psi$.

AN EXAMPLE FOR OPTION FILE